

# Magnetic phase separation and cluster-spin-glass behavior in $\text{LaMn}_{1-x}\text{Fe}_x\text{O}_{3+y}$

O. F. de Lima,<sup>1,a)</sup> J. A. H. Coaquira,<sup>2</sup> R. L. de Almeida,<sup>1,3</sup> and S. K. Malik<sup>3</sup>

<sup>1</sup>*Instituto de Física Gleb Wataghin, UNICAMP, 13083-970 Campinas, Sao Paulo, Brazil*

<sup>2</sup>*Núcleo de Física Aplicada, Instituto de Física, UnB, 70910-970 Brasília, Distrito Federal, Brazil*

<sup>3</sup>*Centro Internacional de Física da Matéria Condensada, UnB, 70904-970 Brasília, Distrito Federal, Brazil*

(Presented 22 January 2010; received 27 October 2009; accepted 17 January 2010; published online 21 April 2010)

The crystal structure and some magnetic properties were investigated for polycrystalline samples of  $\text{LaMn}_{1-x}\text{Fe}_x\text{O}_{3+y}$ , prepared by solid-state reaction in air. All samples show the ORT-2 orthorhombic structure that suppresses the Jahn–Teller distortion and favors a ferromagnetic (FM) superexchange interaction between  $\text{Mn}^{3+}\text{–O–Mn}^{3+}$ . An evolution from a fairly strong FM phase, for  $x=0.0$ , to an antiferromagnetic (AFM) phase, for  $x=1.0$ , was observed. For intermediate Fe contents, a magnetic mixed-phase state occurs, with a gradual decrease (increase) in the FM (AFM) phase as  $x$  increases. A clear cluster-spin-glass (CG) behavior is observed in our samples for  $x \leq 0.1$ , where FM coupling dominates. In this case, the Vogel–Fulcher law describes very well the CG dynamics, giving reasonable values for the fitted parameters. © 2010 American Institute of Physics.

[doi:10.1063/1.3364056]

## I. INTRODUCTION

Substitutions on the Mn site of  $\text{LaMnO}_3$ , by various 3d cations (e.g., Cr, Co, Ni, and Fe), has been explored in the past years.<sup>1–5</sup> Recently, we reported on the crystal structure and magnetic properties of polycrystalline  $\text{LaMn}_{1-x}\text{Fe}_x\text{O}_{3+y}$  ( $0.0 \leq x \leq 1.0$ ) samples, prepared by solid state reaction in air.<sup>6</sup> These samples are single phase and show an ORT-2 orthorhombic structure<sup>7,8</sup> that suppresses the Jahn–Teller distortion, thus favoring a ferromagnetic (FM) superexchange (SE) interaction between<sup>9</sup>  $\text{Mn}^{3+}\text{–O–Mn}^{3+}$ . Because the samples were reacted in air they have an oxygen excess<sup>7,8,10</sup> of  $y \approx 0.09$ , which produces vacancies in the La and Mn sites. For a sample with  $x=0$  this generates a fraction around 18% of  $\text{Mn}^{4+}$  ions and 82% of the usual  $\text{Mn}^{3+}$  ions, with possible double-exchange interaction between them. We have found<sup>6</sup> an evolution from a strong FM phase with a Curie temperature  $T_C \sim 160$  K, for  $x=0.0$ , to an antiferromagnetic (AFM) phase with  $T_N=790$  K, for  $x=1.0$ , accompanied by signs of cluster-spin-glass (CG) behavior and superparamagnetism. Since the Fe doping in  $\text{LaMn}_{1-x}\text{Fe}_x\text{O}_{3+y}$  is known to produce only stable  $\text{Fe}^{3+}$  ions,<sup>3,11</sup> the suppression of ferromagnetism while  $x$  increases can be related to the gradual substitution of  $\text{Mn}^{3+}$  by  $\text{Fe}^{3+}$ , which reduces the amount of DE-coupled  $\text{Mn}^{4+}\text{–O–Mn}^{3+}$  bonds. Here we will present more detailed data and discussions concerning the cluster-glass behavior in the same set of  $\text{LaMn}_{1-x}\text{Fe}_x\text{O}_{3+y}$  samples.

## II. EXPERIMENTAL DETAILS

A set of  $\text{LaMn}_{1-x}\text{Fe}_x\text{O}_{3+y}$  samples, with  $0.0 \leq x \leq 1.0$ , was reacted using the solid diffusion method in open air.<sup>6</sup> For each sample we started with the stoichiometric mixture of

$\text{La}(\text{OH})_3$ ,  $\text{Mn}_2\text{O}_3$ , and  $\text{Fe}_2\text{O}_3$  powders, which was fired in a tubular furnace at the temperature of 1100 °C, for 24 h. The prereacted material was crushed and milled. Then the powder was pressed into a cylindrical sample that was returned to the furnace for a reaction and sintering treatment, at 1100 °C for 24 h. After the sample preparation, small pieces with masses in the range of 20–80 mg were cut for the magnetic measurements with a superconducting quantum interference device magnetometer, model MPMS-5T, and a PPMS-9T system, both from Quantum Design.

X-ray spectra were measured with a Phillips powder-diffractometer, at room temperature and using Cu  $K\alpha$  radiation. Rietveld analysis of the diffraction patterns indicated that all samples contain at least 90% of pure manganite phase, with an orthorhombic structure (space group  $Pnma$ ). The calculated lattice parameters for the sample with  $x=0.0$  are  $a=5.535$  Å,  $b=7.786$  Å, and  $c=5.500$  Å, within the expected values that characterize the so-called O-type orthorhombic structure (ORT-2),<sup>7,8</sup> where  $c < b/2^{1/2} < a$ . This structure suppresses the Jahn–Teller distortion, which involves a cooperative rotation of the  $\text{MnO}_6$  octahedras and favors an isotropic FM SE-interaction<sup>9</sup> between  $\text{Mn}^{3+}\text{–O–Mn}^{3+}$ .

## III. RESULTS AND DISCUSSIONS

Figures 1(a) and 1(b) show some magnetization curves for several samples and ac susceptibility (ACS) data for sample  $x=0.0$ , using several frequencies for the excitation field  $h=1$  Oe. All measurements were performed under a constant magnetic field  $H=100$  Oe. Sharp FM-like transitions were found for small Fe contents ( $x \leq 0.1$ ), becoming broader, weaker, and shifted to lower temperatures for higher  $x$  values. Figure 2 shows the ACS data for samples  $x=0.1$  and 0.5, although similar measurements were also taken for the other compositions. For  $x \leq 0.1$ , the ACS curves show a

<sup>a)</sup>Electronic mail: delima@ifi.unicamp.br.

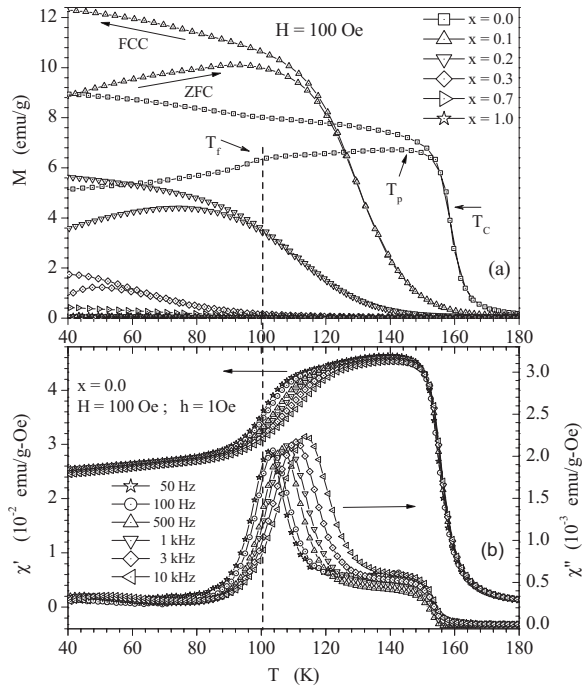


FIG. 1. (a) Magnetization and (b) ACS as a function of temperature, measured under constant magnetic field  $H=100$  Oe. The Curie ( $T_C$ ), blocking ( $T_p$ ), and freezing ( $T_f$ ) temperatures for the cluster-glass system are indicated in (a). The measurements shown in (b) were made in sample  $x=0.0$  with an excitation field  $h=1$  Oe.

frequency dependent (independent) maximum at  $T_f$  ( $T_p$ ) in the imaginary components, accompanied by a corresponding inflexion points in the real components.  $T_p$  is an average blocking temperature where the clusters moments begin to freeze, and  $T_f(\nu)$  is the freezing temperature where this ther-

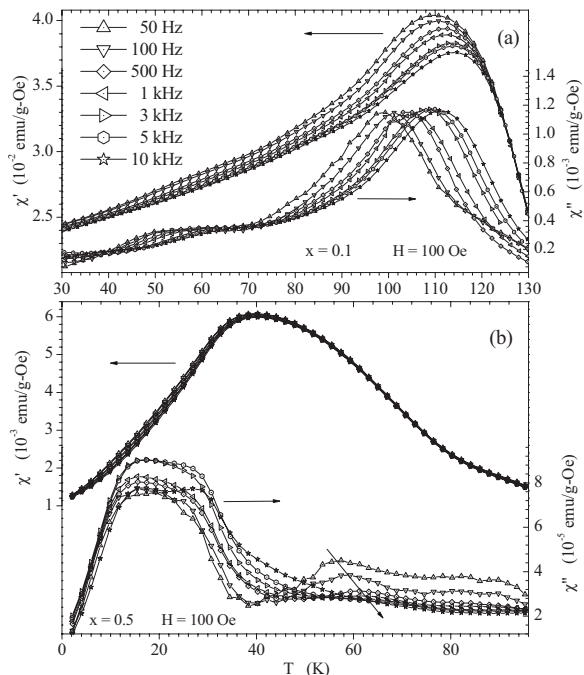


FIG. 2. ACS as a function of temperature, measured under constant magnetic field  $H=100$  Oe and excitation field  $h=1$  Oe: (a) sample  $x=0.1$  that shows strong cluster-glass behavior for  $T < T_C \approx 133$  K; (b)  $x=0.5$  that shows a weak cluster-glass behavior for  $T \geq T_C \approx 64$  K.

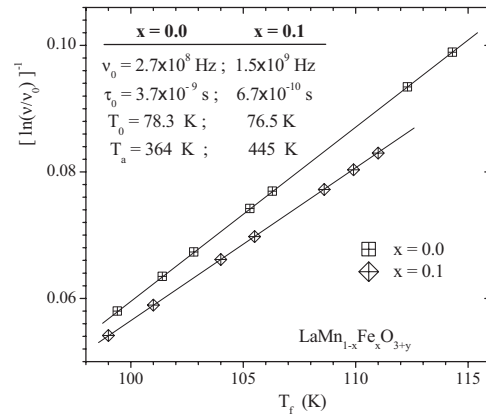


FIG. 3. The solid straight lines represent good tests of the VF law for samples  $x=0.0$  and  $0.1$ . The relaxation time ( $\tau_0=1/\nu_0$ ), activation energy ( $E_a=k_B T_a$ ), and intercluster interaction temperature ( $T_0$ ) show fitted values suitable for a CSG system.

mally activated process reaches a maximum. Possibly the clusters consist of FM or FM-like islands embedded in an AFM matrix.<sup>6,9</sup> This would be consistent with the fact that  $T_p$  and  $T_f$  are always smaller than  $T_C$  for samples with  $x \leq 0.1$ . Another consistent feature is the observed strong irreversibility between ZFC and FCC magnetization curves, typical for relaxation phenomena in CG systems.<sup>12-14</sup>

As shown in Fig. 3,  $T_f(\nu)$  follow very well a CG dynamics described by the Vogel-Fulcher (VF) law,<sup>15</sup>  $\ln(\nu/\nu_0) = -E_a/k_B(T_f - T_0)$ , where  $k_B$  is the Boltzmann constant. Then,  $T_f$  is connected with the ratio between the ACS measuring frequency  $\nu$  and the system attempt frequency  $\nu_0=1/\tau_0$ , where  $\tau_0$  is a characteristic relaxation time.  $E_a=k_B T_a$  is an activation energy and  $T_0$  is a temperature usually related to the intercluster magnetic energy.<sup>15</sup> These parameters, calculated from the best fittings of the VF law, have values consistent with a CG system as shown in the inset of Fig. 3 for samples  $x=0.0$  and  $0.1$ . For a canonical spin glass (SG), it would be expected that<sup>15,16</sup>  $\tau_0 > 10^{-4}$  s and  $t^*=(T_f - T_0)/T_f < 0.1$ , while for CG typically  $\tau_0 < 10^{-7}$  s and  $t^* \geq 0.5$ . Our values of  $t^* \approx 0.3$  are smaller than  $0.5$  but still acceptable for a CG, since much smaller values must be expected for an ideal SG.

The ratio  $T_a/T_f$  found in our samples are around  $3(x=0.0)$  and  $4(x=0.1)$ , in close agreement with the results for a  $\text{LaMn}_{1-x}\text{Mg}_x\text{O}_3$  system.<sup>17</sup> The fact that  $T_a$  increases with  $x$  indicates that higher activation energy would be required to observe a CG behavior in samples with higher iron contents. Possibly this explains why the CG features for  $T < T_C$  were not observed for the samples with  $x \geq 0.3$ , in our experimental conditions. On the other hand, it is worth noticing that smaller frequency-dependent peaks in  $\chi''$  appear around 56 K, for both  $x=0.1$  and  $0.5$  samples (Fig. 2). However this happens around and above  $T_C$  for sample  $x=0.5$ , and possibly these peaks are related to the dynamics of another spin system existing in the sample. For instance, a likely candidate could be the cluster system formed by a canted component of the AFM phase that grows as  $x$  increases.<sup>6</sup> We are analyzing this possibility and the results will be published elsewhere.

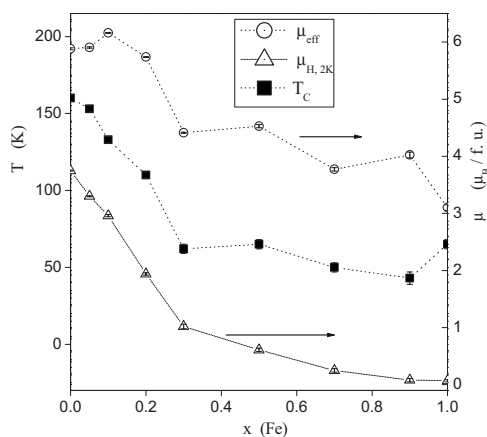


FIG. 4. Some magnetic properties plotted as a function of iron content  $x$ . The effective magnetic moment ( $\mu_{\text{eff}}$ ) and saturation moment at 2 K ( $\mu_{\text{H},2\text{K}}$ ) refer to the right axis, in units of  $\mu\text{B}/\text{f.u.}$  The Curie temperature ( $T_{\text{C}}$ ) refers to the left axis. The lines are only a guide to the eye.

The Curie temperature ( $T_{\text{C}}$ ) and effective magnetic moment ( $\mu_{\text{eff}}$ ) were calculated for each sample, using the  $M(T)$  data [Fig. 1(a)]. In addition, the saturation moment at 2 K ( $\mu_{\text{H},2\text{K}}$ ) was determined from  $M(H)$  curves for  $|H| \leq 50$  kOe (not shown). In general, all these properties decrease their values while the iron content ( $x$ ) increases, as shown in Fig. 4. This has been interpreted<sup>6</sup> as an evolution of the magnetic phases that starts in  $x=0.0$  with a FM behavior, due to  $\text{Mn}^{3+}\text{-O-Mn}^{4+}$  double-exchange and  $\text{Mn}^{3+}\text{-O-Mn}^{3+}$  SE couplings. Then, by increasing  $x$  the system evolves to a FM-like behavior, mainly caused by a canted-antiferromagnetism originated from a gradual increase of  $\text{Fe}^{3+}\text{-O-Fe}^{3+}$  bonds. Since the compound  $\text{LaFeO}_{3+y}$  ( $x=1.0$ ) is known to present an AFM coupling with spin canting,<sup>18</sup> possibly this could be the origin for the observed weak ferromagnetism in our samples.

#### IV. CONCLUSIONS

Polycrystalline samples of  $\text{LaMn}_{1-x}\text{Fe}_x\text{O}_{3+y}$  ( $0.0 \leq x \leq 1.0$ ) were prepared using the solid diffusion reaction method. X-ray diffraction data and Rietveld analysis indicated that our samples contain at least 90% of the manganite phase, all them having orthorhombic structure (space group  $Pnma$ ). Since the samples were reacted in air we estimated an oxygen excess of  $y=0.09$ , and occurrence of the ORT-2 type of orthorhombic structure, where  $c < b/2^{1/2} < a$ , with lattice parameters  $a=5.535$  Å,  $b=7.786$  Å, and  $c=5.500$  Å ( $x=0.0$ ).

Magnetization and ACS measurements allowed a thorough characterization of the magnetic properties at low and high temperatures. In general the Curie temperature ( $T_{\text{C}}$ ), the

effective magnetic moment ( $\mu_{\text{eff}}$ ), and the saturation moment at 2 K ( $\mu_{\text{H},2\text{K}}$ ) decrease, while the iron content ( $x$ ) increases. This was interpreted as an evolution of the magnetic phases that starts at  $x=0.0$  with a FM behavior, due to  $\text{Mn}^{3+}\text{-O-Mn}^{4+}$  double-exchange and  $\text{Mn}^{3+}\text{-O-Mn}^{3+}$  SE couplings. Following, it evolves to a FM-like behavior, mainly caused by a canted-antiferromagnetism originated from a gradual increase of  $\text{Fe}^{3+}\text{-O-Fe}^{3+}$  bonds.

Unambiguous CG behavior is observed in our samples for  $x \leq 0.1$ , where FM coupling dominates. In this region, the VF law describes our data very well, giving reasonable values for the fitted parameters. For higher Fe contents a magnetic mixed-phase state occurs, with gradual decrease (increase) in ferromagnetism (antiferromagnetism), leading to the CG suppression below  $T_{\text{C}}$ .

#### ACKNOWLEDGMENTS

We acknowledge the financial support from Brazilian science agencies Fundação de Amparo à Pesquisa do Estado de São Paulo (FAPESP), Conselho Nacional de Desenvolvimento Científico e Tecnológico (CNPq), and Coordenação de Aperfeiçoamento de Pessoal de Nível Superior (CAPES). We thank C. A. Cardoso for helpful discussions and also thank A. Ferraz and S. Quezado for their interest on this work.

- <sup>1</sup>K. H. Ahn, X. W. Wu, K. Liu, and C. L. Chien, *Phys. Rev. B* **54**, 15299 (1996).
- <sup>2</sup>R. Mahendiran, B. Raveau, M. Hervieu, C. Michel, and A. Maignan, *Phys. Rev. B* **64**, 064424 (2001).
- <sup>3</sup>W. Tong, B. Zhang, S. Tan, and Y. Zhang, *Phys. Rev. B* **70**, 014422 (2004).
- <sup>4</sup>K. De, R. Ray, R. N. Panda, S. Giri, H. Nakamura, and T. Kohara, *J. Magn. Magn. Mater.* **288**, 339 (2005).
- <sup>5</sup>K. De, M. Patra, S. Majumdar, and S. Giri, *J. Phys. D: Appl. Phys.* **40**, 7614 (2007).
- <sup>6</sup>O. F. de Lima, J. A. H. Coaquira, R. L. de Almeida, L. B. de Carvalho, and S. K. Malik, *J. Appl. Phys.* **105**, 013907 (2009).
- <sup>7</sup>B. Hauback, H. Fjellvag, and N. Sakai, *J. Solid State Chem.* **124**, 43 (1996).
- <sup>8</sup>Q. Huang, A. Santoro, J. W. Lynn, R. W. Erwin, J. A. Borchers, J. L. Peng, and R. L. Greene, *Phys. Rev. B* **55**, 14987 (1997).
- <sup>9</sup>J. Töpfer and J. B. Goodenough, *J. Solid State Chem.* **130**, 117 (1997).
- <sup>10</sup>J. M. D. Coey, M. Viret, and S. von Molnár, *Adv. Phys.* **48**, 167 (1999).
- <sup>11</sup>S. D. Bhame, V. L. Joseph Joly, and P. A. Joy, *Phys. Rev. B* **72**, 054426 (2005).
- <sup>12</sup>P. C. Hohenberg and B. I. Halperin, *Rev. Mod. Phys.* **49**, 435 (1977).
- <sup>13</sup>F. M. Araújo-Moreira, W. A. Ortiz, and O. F. de Lima, *Physica C* **311**, 98 (1999).
- <sup>14</sup>R. S. Freitas, L. Ghivelder, F. Damay, F. Dias, and L. F. Cohen, *Phys. Rev. B* **64**, 144404 (2001).
- <sup>15</sup>J. A. Mydosh, *Spin Glasses: An Experimental Introduction* (Taylor and Francis, London, 1993).
- <sup>16</sup>S. Mukherjee, R. Ranganathan, P. S. Anilkumar, and P. A. Joy, *Phys. Rev. B* **54**, 9267 (1996).
- <sup>17</sup>J. Blasco, J. García, G. Subías, and M. C. Sánchez, *Phys. Rev. B* **70**, 094426 (2004).
- <sup>18</sup>M. Eibschütz, S. Shtrikman, and D. Treves, *Phys. Rev.* **156**, 562 (1967).